

Supplementary Material

Experimental and numerical studies of fine quartz particle sedimentation based on particle morphology

Chunfu Liu^{1,*}, Kai Lv², Lingyun Liu¹, Jun Chen¹, Bao Ren¹, XueJie Bai³ and Fanfei Min^{1,*}

¹ Department of Materials Science and Engineering, Anhui University of Science and Technology, Huainan 232001, China

² Hefei Gotion High-tech Power Energy Co., Ltd, Hefei, Anhui 230000, China

³ School of Chemical Engineering and Technology, China University of Mining and Technology, Xuzhou, Jiangsu 221116, China

* Corresponding author: Tel: +86-554-6668885, Fax: +86-554-6668885

E-mail address: ffmin@aust.edu.cn; chfuliu@aust.edu.cn

The quartz samples were processed by wet sieve with 30 mesh, 60 mesh, 120 mesh, 200 mesh, 325 mesh and 500 mesh series. Then, each classified sample was mixed with hydrogen peroxide. After standing for 24 hours, the water was heated to 60°C, the objective being to decompose the remaining hydrogen peroxide and remove impurities. The processed samples were dried at 60°C and bottled for later use.

X-ray fluorescence (XRF) and X-ray diffraction (XRD) analyses were carried out on the treated samples, and the results are shown in Table 1 and Figure1. The results show that the purity of the treated samples meet the requirements of the experiment.

Table S1. XRF analysis of quartz.

Component	Na ₂ O	MgO	Al ₂ O ₃	SiO ₂	P ₂ O ₅	SO ₃	K ₂ O	CaO	TiO ₂	Fe ₂ O ₃
proportion (%)	0	0.34	0.5	96.49	0.08	0.12	0	0	0.35	2.12

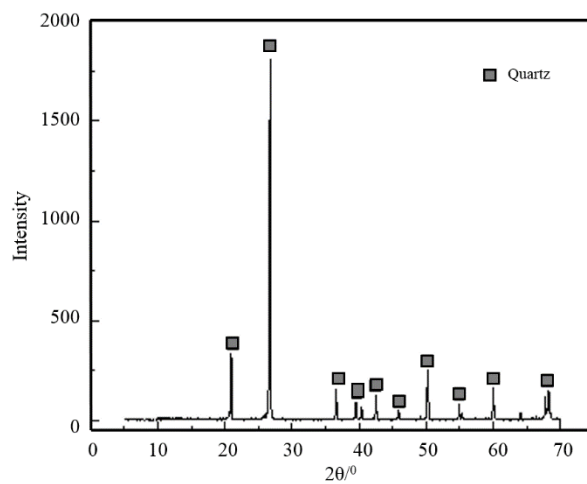


Figure S1. XRD analysis of quartz.

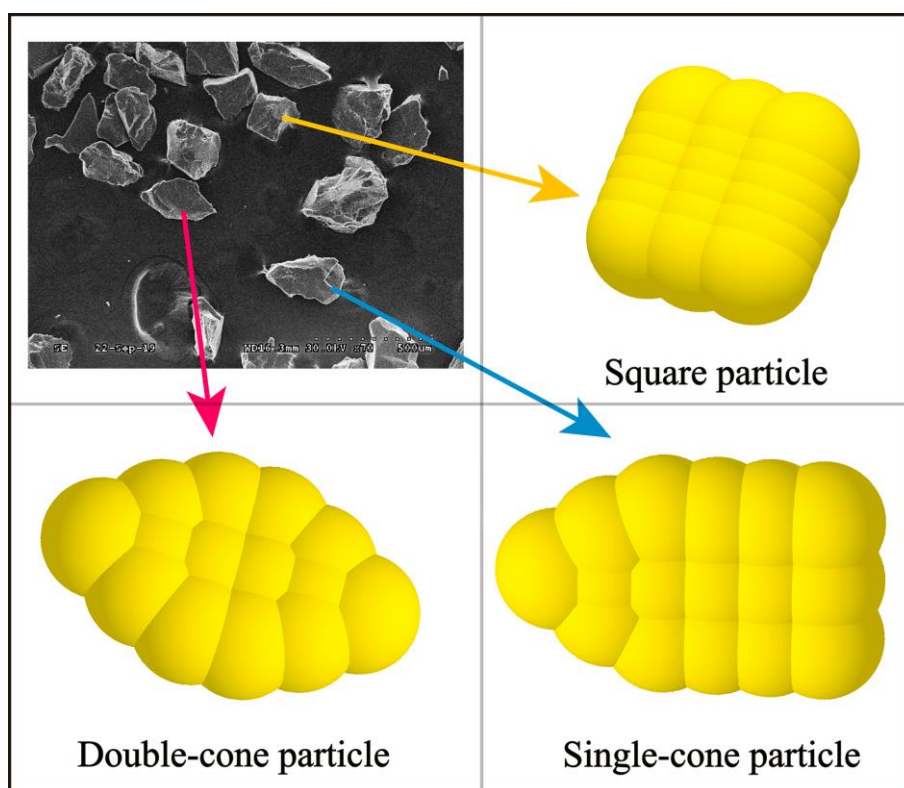


Figure S2. Schematic diagram of particle peripheral morphology definition and simplified model

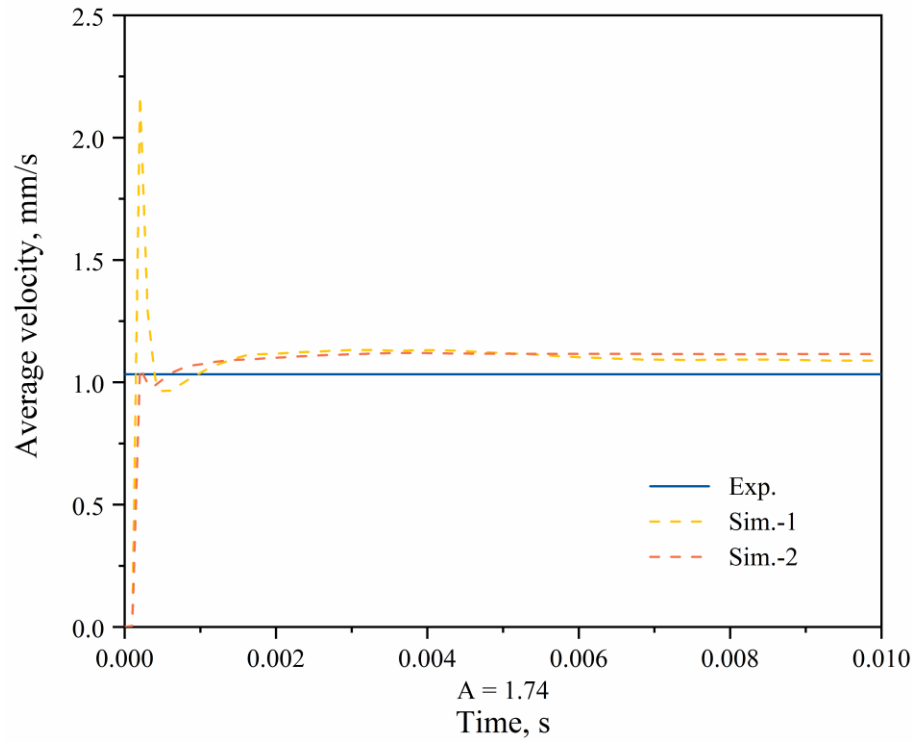


Figure S3. The instantaneous velocities of particles changes when the length is $56\text{ }\mu\text{m}$ and the width is $32\text{ }\mu\text{m}$.

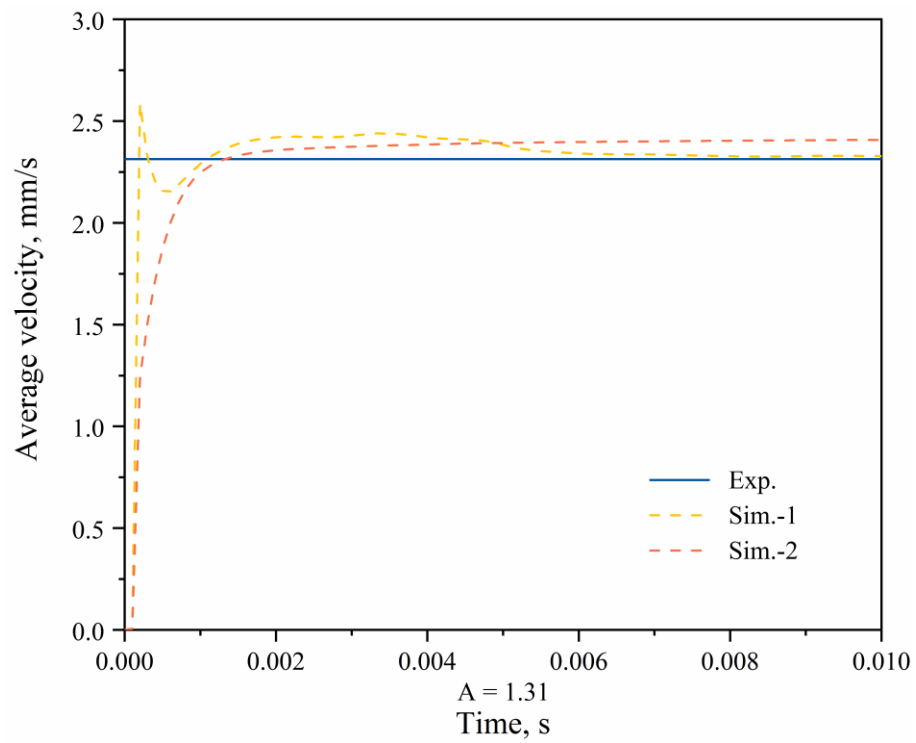


Figure S4. The instantaneous velocities of particles changes when the length is $68\text{ }\mu\text{m}$ and the width is $52\text{ }\mu\text{m}$.

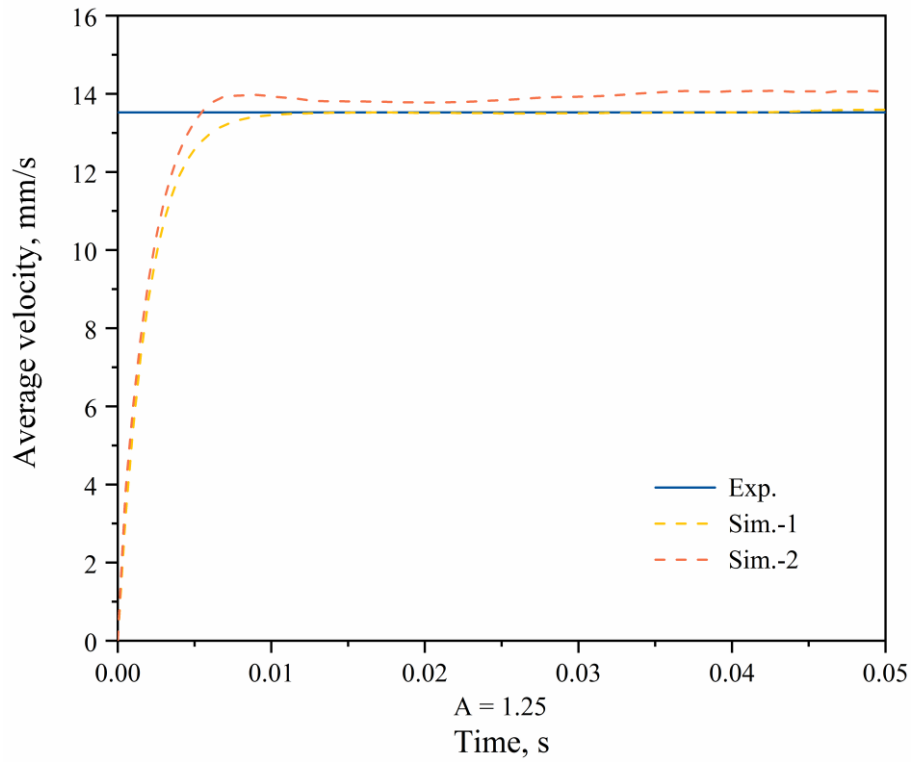


Figure S5. The instantaneous velocities of particles changes when the length is 168 μm and the width is 135 μm .

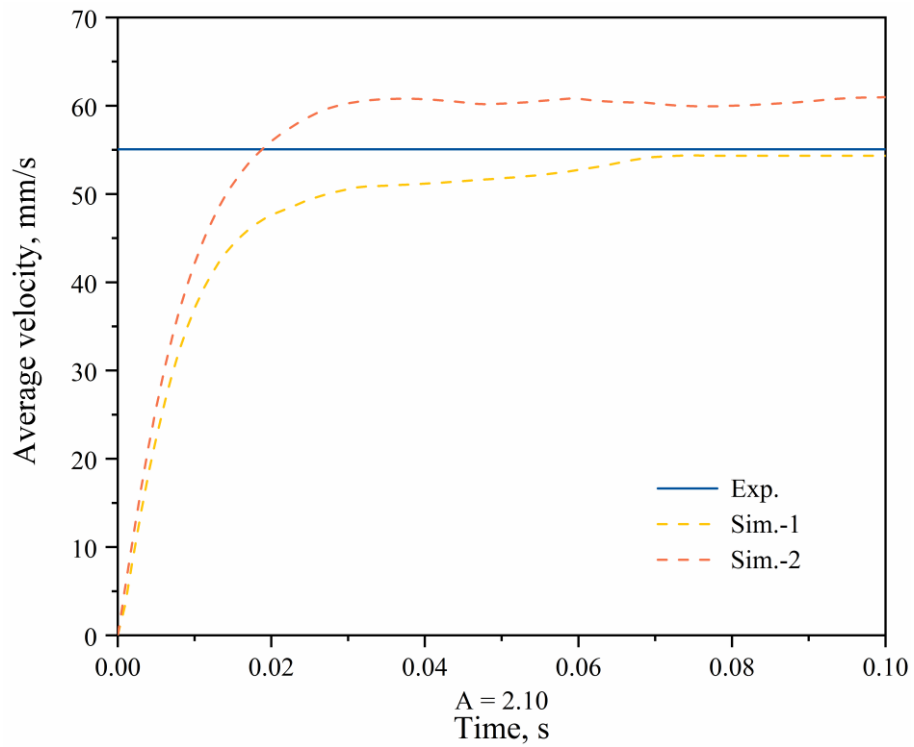


Figure S6. The instantaneous velocities of particles changes when the length is 712 μm and the width is 339 μm .

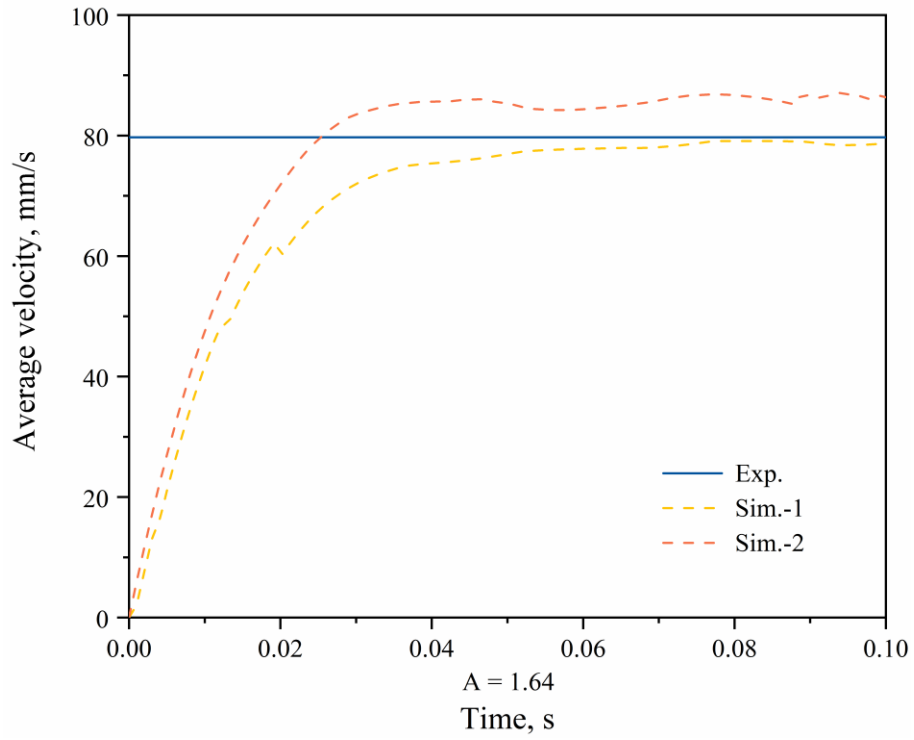


Figure S7. The instantaneous velocities of particles changes when the length is $777 \mu\text{m}$ and the width is $473 \mu\text{m}$.

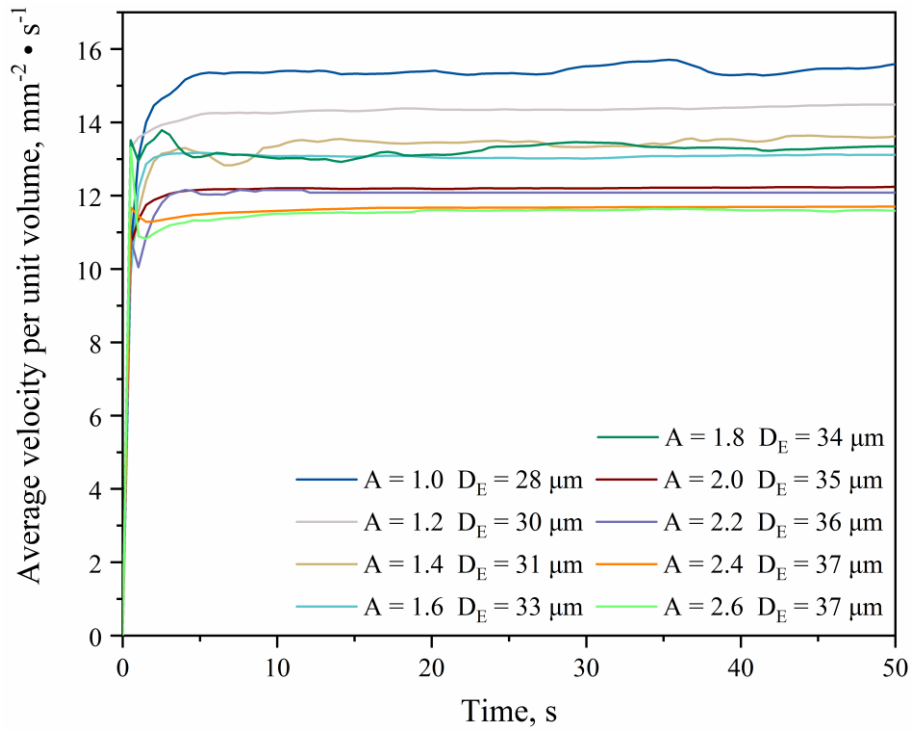


Figure S8. Instantaneous velocities of particles with different long-middle axis ratios in an effective particle size of about $30 \mu\text{m}$.

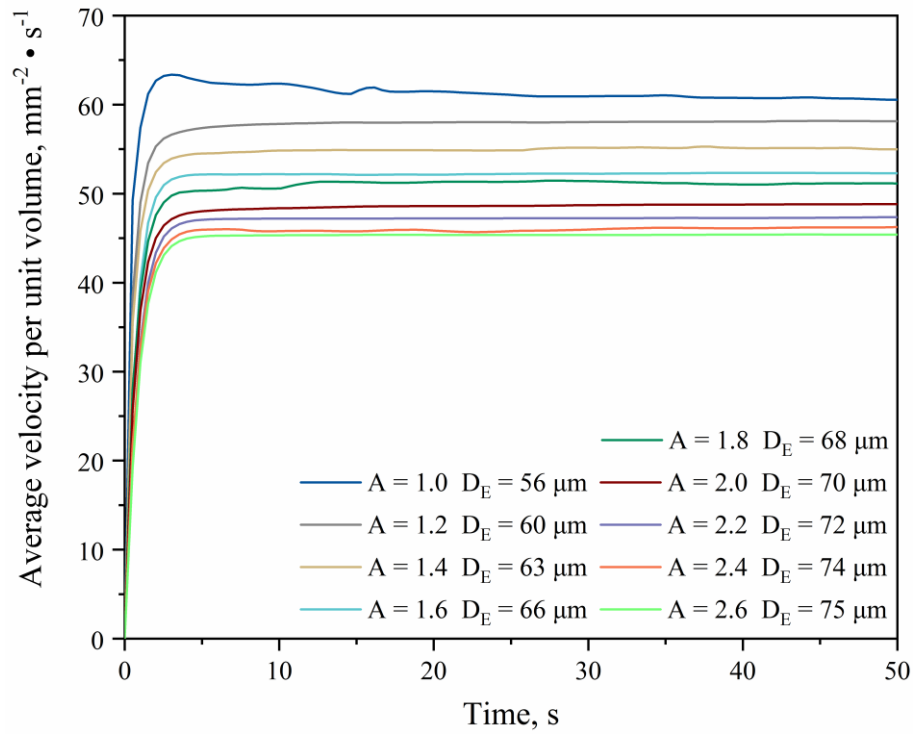


Figure S9. Instantaneous velocities of particles with different long-middle axis ratios in an effective particle size of about 60 μm .

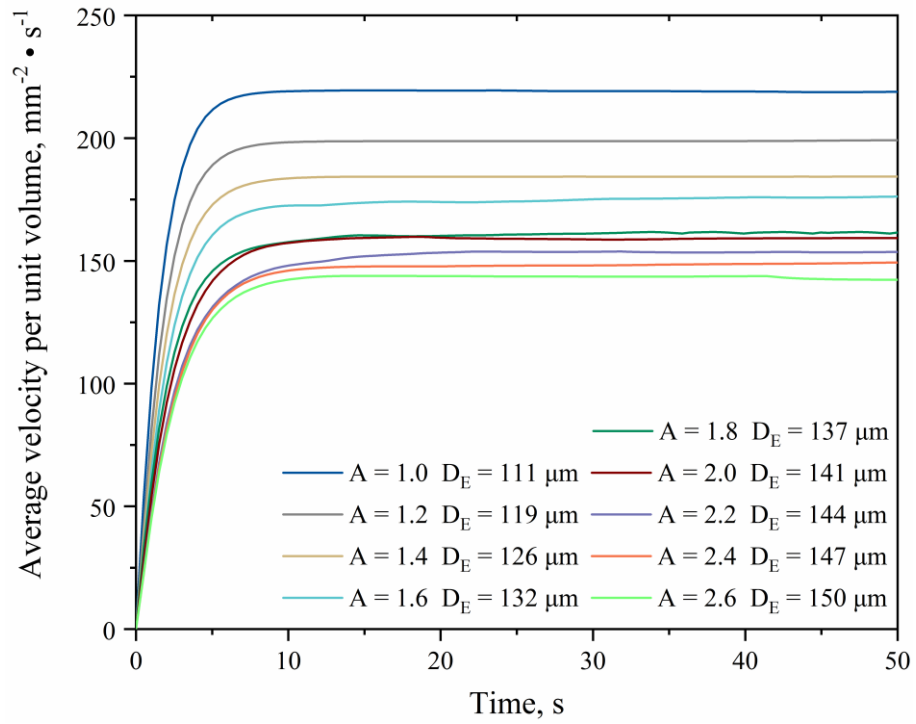


Figure S10. Instantaneous velocities of particles with different long-middle axis ratios in an effective particle size of about 125 μm .

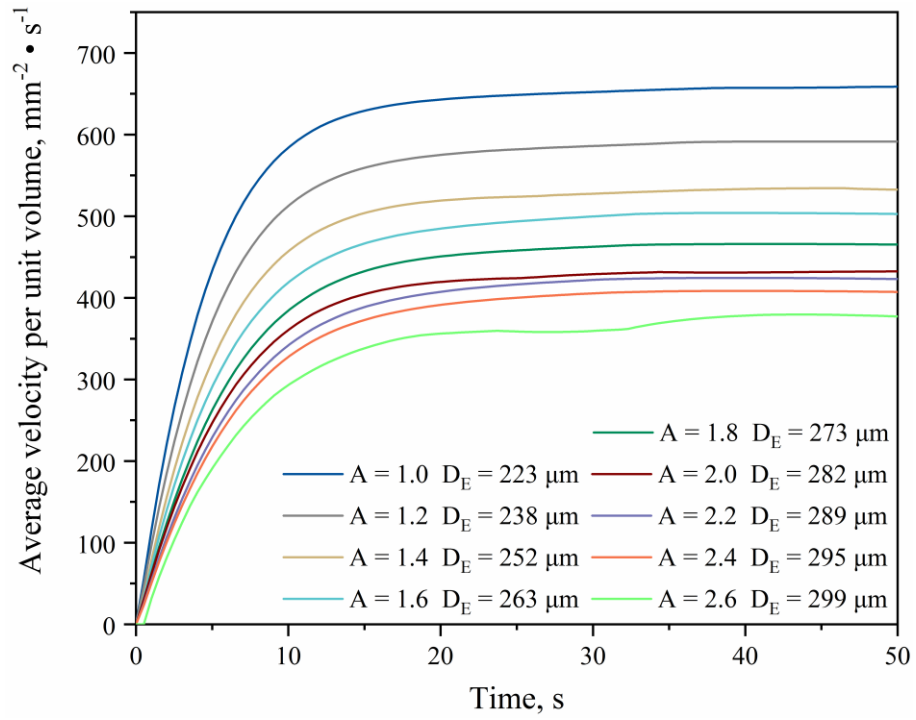


Figure S11. Instantaneous velocities of particles with different long-middle axis ratios in an effective particle size of about $250 \mu\text{m}$.

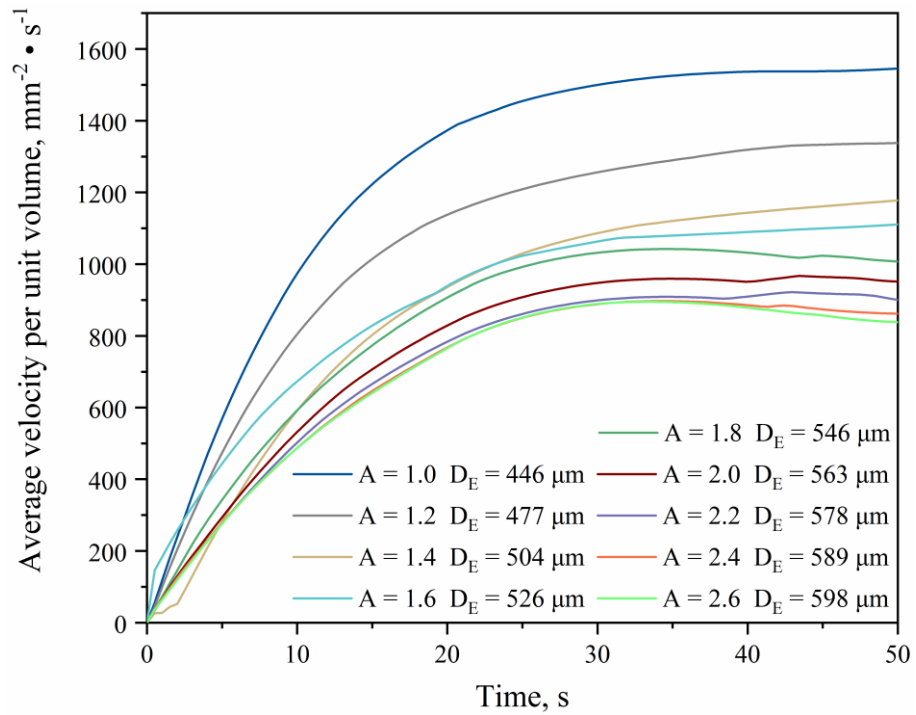


Figure S12. Instantaneous velocities of particles with different long-middle axis ratios in an effective particle size of about $500 \mu\text{m}$.